Influence of surface charge, binding site residues and glycosylation on *Thielavia terrestris* cutinase biochemical characteristics

Abhijit N. Shirke[1,2], **Danielle Basore**[2,3], **Samantha Holton**[2,4], **An Su**[1,2], **Evan Baugh**[5], **Glenn L. Butterfoss**[6], **George Makhatadze**[1,2,3], **Christopher Bystroff**[2,3,7], and **Richard A. Gross**[1,2,3]

Christopher Bystroff: bystrc@rpi.edu; Richard A. Gross: grossr@rpi.edu

[1]Department of Chemistry and Chemical Biology, Rensselaer, Polytechnic Institute, CBIS 4105, 110 8th Street, Troy, NY 12180, USA

[2]Center for Biotechnology and Interdisciplinary Studies, Rensselaer Polytechnic Institute, Troy, NY, USA

[3]Department of Biological Sciences, Rensselaer Polytechnic Institute, J-Rowl, 3C07, 110 8th Street, Troy, NY 12180, USA

[4]Department of Biomedical Engineering, Rensselaer Polytechnic Institute, Troy, NY, USA

[5]Center for Genomics and Systems Biology, New York University, New York, NY, USA

[6]Center for Genomics and Systems Biology, New York University Abu Dhabi, Abu Dhabi, United Arab Emirates

[7]Department of Computer Science, Rensselaer Polytechnic Institute, Troy, NY, USA

Abstract

Cutinases are esterases of industrial importance for applications in recycling and surface modification of polyesters. The cutinase from *Thielavia terrestris* (TtC) is distinct in terms of its ability to retain its stability and activity in acidic pH. Stability and activity in acidic pHs are desirable for esterases as the pH of the reaction tends to go down with the generation of acid. The pH stability and activity are governed by the charged state of the residues involved in catalysis or in substrate binding. In this study, we performed the detailed structural and biochemical characterization of TtC coupled with surface charge analysis to understand its acidic tolerance. The stability of TtC in acidic pH was rationalized by evaluating the contribution of charge interactions to the Gibbs free energy of unfolding at varying pHs. The activity of TtC was found to be limited by substrate binding affinity, which is a function of the surface charge. Additionally, the presence of glycosylation affects the biochemical characteristics of TtC owing to steric interactions with residues involved in substrate binding.

Compliance with ethical standards This article does not contain any studies with human participants or animals performed by any of the authors.

Conflict of interest The authors declare that they have no conflict of interest.

Keywords

Cutinase; Surface charge; Substrate binding; Glycosylation; Biochemical characterization; Polyester hydrolysis

---

Introduction

Cutinases are esterases that have a relatively accessible catalytic triad, allowing them to act on rigid polymer substrates and cleave ester bonds in complex molecules (Martinez et al. 1992). In nature, they act as the attacking machinery for phytopathogenic microorganisms (fungi and bacteria), facilitating the breakdown of the protective plant layer cutin, a complex biopolyester (Purdy and Kolattukudy 1975).

Cutinases have been explored for a number of applications that include polymer recycling (Mueller 2006), polymer degradation (Bhardwaj et al. 2012), polymer surface modification of textiles (Matamá et al. 2009) and biomaterials (Guebitz and Cavaco-Paulo 2008) and lipolytic activity in detergents (Dutta et al. 2009). Apart from their esterase activity on polymeric substrates, cutinases also catalyze esterification and transesterification reactions on low molecular weight substrates (Hunsen et al. 2007; De Barros et al. 2012) (Badenes et al. 2010).

Cutinases from a variety of microbial sources (fungal and bacterial) have been identified and characterized with several crystal structures of homologues deposited in Protein Data Bank (3GBS, 1CEX, etc). They are alpha/beta hydrolases with a canonical catalytic triad of serine, aspartic acid, and histidine. Cutinase-catalyzed hydrolysis or transesterification reactions progress through the formation of a tetrahedral carbon intermediate (Köller and Kolattukudy 1982), which is stabilized by an oxyanion hole constituted by residues such as Q121 and S42 in *Fusarium solani* cutinase (FsC) (Martinez et al. 1994). *F. solani* cutinase (FsC) is most extensively studied, including comprehensive stability analysis and biochemical characterization for different applications. Additionally, protein engineering of FsC has led to the development of a number of variants better suited to various conditions and substrates (Chen et al. 2013). Several cutinases with biochemical properties attractive for a variety of applications have been identified and tested. However, there is a dearth of good comparative studies of these homologues. For example, our group found that a cutinase from *Aspergillus oryzae* (AoC) possesses better activity on poly(ε-caprolactone), PCL, than FsC, which was attributed to the presence in AoC of an extended catalytical groove near the active site (Liu et al. 2009). We also reported that for polyethylene terephthalate (PET) hydrolysis and polyvinyl acetate deacetylation, the engineered cutinase from *Humicola insolens* (HiC) developed by Novozymes has higher catalytic efficiency than wt-FsC and a cutinase from *Pseudomonas mendocina* (PmC) (Ronkvist et al. 2009a, b). Cutinases from thermophilic bacteria such as *Thermobifida fusca* (T_m = 70 °C) (Roth et al. 2014), *Thermobifida alba* (T_m = 70 °C) (Hu et al. 2010) and *Saccharomonospora viridis* (T_m = 70 °C) (Kawai et al. 2014) are relatively more thermostable than the fungal cutinases FsC, PmC, AoC and HiC. Furthermore, these thermophilic bacteria derived cutinases and are known to have PET hydrolysis activity. These enzymes are structurally distinct from FsC but do have structural

homology to lipases from the genus *Streptomyces*. Recently, a cutinase isolated from leaf and branch compost with structural similarity to *T. alba* cutinase was characterized and found to be highly thermostable ($T_m = 86\ °C$) (Sulaiman et al. 2012, 2014).

Cutinase from *Thielavia terrestris* (TtC) is notable for its activity in acidic environments where other cutinases lose stability and activity (Yang et al. 2013). This is advantageous as it permits TtC to retain its enzymatic activity during polyester hydrolysis reactions where the solution pH decreases as increased quantities of water-soluble hydroxyacids and/or di-acids are formed. Yang et al. studied TtC catalysis on polymeric substrates and showed that its activity exhibits a broad pH optimum that extends well into the acidic range (4 to 8). TtC is also reported to be more structurally stable at acidic pHs, but the structural basis for this stability is not understood (Yang et al. 2013). Recently, cutinases from *Aspergillus niger* (AnC) (Nyyssölä et al. 2013) and *Sirococcus conigenus* (SsC) (Nyyssölä et al. 2014) were also found to be active and stable under acidic pH conditions. AnC has a narrow pH optimum range (pH 5–6) whereas SsC's pH optimum range is broad, extending from pH 3 to 7. However, both enzymes are thermally less stable than TtC (Nyyssölä et al. 2013, 2014; Yang et al. 2013).

The pH often has dramatic effects on protein stability and activity. Changes in amino acid protonation state often alter electrostatic interactions and spatial arrangements in the protein structure (Horng et al. 2005; Mazzini et al. 2007). Thus, thermostability at a particular pH can be explained by effects of electrostatics on the free energy. Electrostatic or surface charge analysis has been successfully used to predict protein stability and to design thermostable variants (García-Mayoral et al. 2006; Gribenko et al. 2009; Chan et al. 2012). Furthermore, the effects of pH on secondary and tertiary structure stability have been well studied and, often, conformational changes associated with shifts in pH correlate to changes in protein function and activity (Talley and Alexov 2010). However, changes in the protonation state of active site residues (Sussman et al. 2013; Sampogna and Honig 1994; Banás et al. 2010) and the pH effects on substrate binding (Yamato and Rosenbusch 1983; Jehle et al. 2010) may contribute to a pH-activity profile without significant changes in protein structure. For example, in cutinases, the negative electrostatic potential at the active site required for optimal activity may be affected by pH (Neves-Petersen et al. 2001).

Interfacial substrate binding is essential for increased enzyme concentration on the surface of a polymeric substrate and efficient catalysis. Enzyme binding to polymeric substrates is generally explained by surface adsorption that is a function of electrostatic or hydrophobic interactions of surface amino acid residues with the substrate (Liu et al. 2009; Hiraishi et al. 2010b; Khan et al. 2013). These interactions are pH dependent and, therefore, can influence the pH-activity profile of the enzyme. Additionally, the presence of glycans on the surface of glycosylated proteins can influence substrate binding due to changes in enzyme surface hydrophilicity and steric constraints. Glycans have been shown to affect the substrate binding both positively and negatively based on their size and location (Beckham et al. 2012; Payne et al. 2013; Chen et al. 2014).

This paper presents a detailed structural and biochemical characterization of TtC to understand its stability and activity in acidic environments (pH 5) and evaluates its activity

on polymeric substrates with different surface characteristics (hydrophilic vs hydrophobic). The rationales were clarified by comparison to AoC, which is stable and active in alkaline environment (pH 8). In the absence of TtC's crystal structure, a homology model was developed using AoC's crystal structure as the template. The structural stabilities of proteins were assessed using circular dichroism (CD) and fluorescence analysis. The stability of TtC in acidic pH was rationalized based on surface charge calculations. Substrate binding was correlated with enzyme specificity and to TtC's pH-activity profile. Furthermore, glycosylation was found to indirectly affect substrate binding by sterically affecting important residues for binding. The steric hindrance of an important charged residue (H172) by a glycan results in different pH-activity profiles for the glycosylated and nonglycosylated proteins.

Materials and methods

Materials

Substrate 4-nitrophenyl butyrate (pNPB) and salts monosodium phosphate and disodium phosphate, sodium acetate and sodium borate were purchased from Sigma-Aldrich. Zeocine was purchased from Invitrogen. All the media components used (Liu et al. 2009) were also procured from Sigma-Aldrich. The polymeric substrates polycaprolactone (PCL) (mol wt $Mn = 84,000$) was a gift from DOW. PCL films were casted by the compression molding, and the crystallinity (30– 35 %) was determined using differential scanning calorimetry. Cellulose diacetate (CA) films were obtained form Grafix Plastics, and the degree of substitution of 2 was confirmed by NMR analysis.

Homology modelling

The TtC homology model was developed using the Modeller 2.0 package with the AoC structure (PDB id 3GBS) as the template.

Protein expression and purification

Glycosylated TtC (TtC-G) and AoC were produced by heterologous expression in *Komagataella pastoris* (ATCC 76273) using strong methanol-inducible AoX-1 promoter. The protein (AoC/TtC) was expressed extracellularly with the help of N-terminal *Saccharomyces cerevisiae* alpha factor. A C-terminal histidine tag was incorporated for purification by affinity chromatography. Genes AoC (KT894219) and TtC (KT894218) were cloned in the PJ912 express vector from DNA2.0 and transformed into electrocompetent *K. pastoris* cells using a previously described protocol (Lin-Cereghino et al. 2005). The best-expressing transformant was used for the bulk production of protein (AoC/TtC) using fed batch fermentation at a 4-L scale and purified on a Ni NTA column as reported previously (Liu et al. 2009). Nonglycosylated TtC (TtC-NG) was produced by expression in *E. coli* Dh5α cells. The TtC gene was transformed into DH5α by electroporation using pD881 vector with the rhamnose inducible rhaBAD promoter. The protein was expressed with an N-terminal ompC tag for translocation to the periplasmic membrane. The protein was extracted from cells using ultrasonication and purified using affinity chromatography on Ni NTA column (Online resource 1).

Detection of glycosylation

The glycosylation of TtC was confirmed by glycoprotein staining. Sodium dodecyl sulfate polyacrylamide gel electrophoresis (SDS PAGE) analysis of glycosylated protein was performed under reducing conditions on the 12 % gel. Glycoprotein staining was conducted using Sigma's glycopeptide staining kit (GlycoPro) where glycoproteins are stained magenta. This detection system is a modification of periodic acid-Schiff (PAS) method (Zacharius et al. 1969). After detection of the glycosylated protein, the same gel was stained with Coomassie blue to detect other protein bands. The presence of N-linked glycosylation was further confirmed using the deglycosylating enzyme peptide-N4-(*N*-acetyl-beta-glucosaminyl)asparagine amidase PNGase F (New England Biolabs).

Protein concentration determination

Protein concentrations were measured using the standard BCA method after suitable dilutions (50 μg/mL to 1 mg/mL). Pure protein (TtC/AoC) was used as the standard for calibration curves.

Circular dichroism measurements

CD spectra were recorded using a JASCO J-815 spectropolarimeter coupled with a Peltier-type temperature controller. Stock solutions of cutinase (1 mg/mL) were prepared in (i) 20 mM NaH_2PO_4–H_3PO_4 buffer at pH 3.0, (ii) 20 mM sodium acetate-acetic acid buffer at pH 4.0 and 5.0, (iii) 20 mM Na_2HPO_4–NaH_2PO_4 buffer at pH 6.0, 7.0, 8.0 and (iv) 20 mM sodium borate buffer at pH 9.0 and 10.0. CD analyses were performed using 10 μM protein solutions. To analyze the secondary structure, spectra were recorded from 190 to 250 nm at 25 °C. CD thermal scans from 20 to 80 °C were performed at a heating rate of 1 °C/min and with continuous monitoring of ellipticity changes at 222 nM. Observed ellipticities were transformed to apparent fractions of denatured proteins assuming a two-state deactivation mechanism. The T_m was determined as the midpoint of the unfolding curve at which 50 % of the protein is unfolded.

Fluorescence analysis

Fluorescence analysis was performed using a Spex® Fluorolog® Tau-3 (Hoiba) fluorimeter with slit widths of 2 and 3 nm for the excitation and emission beam, respectively. Protein solutions (2 μM) at the desired pH were used for the analysis. The intrinsic tryptophan fluorescence was recorded from 310 to 550 nm upon excitation at 295 nm. The λ_{max} (wavelength of maximum fluorescence intensity) and the emission intensity at 340 nM were measured for each scan.

Activity measurements

PNPB hydrolysis assay—A standard p-nitrophenyl butyrate (PNPB) hydrolysis assay was used for esterase activity (Baker et al. 2012). The activity at different pHs was measured using different assay buffers (20 mM NaH_2PO_4–H_3PO_4 buffer at pH 3.0, (ii) 20 mM sodium acetate-acetic acid buffer at pH 4.0 and 5.0, (iii) 20 mM Na_2HPO_4–NaH_2PO_4 buffer at pH 6.0, 7.0, 8.0 and (iv) 20 mM sodium borate buffer at pH 9.0 and 10.0). The assay was initiated by addition of PNPB stock solution in methanol (final PNPB concentration of 1

mM) to the diluted 10 nM enzyme solution 85–10 nM in 20 mM pH 8 phosphate buffer. The reaction was monitored by measuring the absorbance at 348 nm using a molecular device spectrophotometer M2. An isosbestic point of PNP at which the absorbance is independent of the pH of the solution is 348 nm (Rhee et al. 2005). One unit of enzyme activity was determined as 1 μM of PNP formed per minute per millilitre of enzyme solution. The PNP molar extinction coefficient at 348 nm ($5207\ M^{-1}cm^{-1}$) was used for activity determinations.

Polymer hydrolysis assay—The cutinase activity for polyester hydrolysis was assayed using a pH-stat apparatus as reported previously with slight modifications (Ronkvist et al. 2009b). The concentration of polymer substrates (CA, PCL) used is 2 cm^2/mL (e.g. the available surface area). The polymeric films were cut into 0.5×0.5 cm pieces. Assays were performed at varying pHs (3–10) and varying temperatures (40–75 °C).

Polymer hydrolysis kinetics—Reaction rates were determined at different enzyme concentrations where the substrate concentration was kept constant at 2 cm^2/mL for both PCL and cellulose acetate (CA) under desired reaction conditions (pH 5 to 8 and temperature 40 °C). The data was fit to the heterogeneous kinetic model developed by Scandola et al. (Eq. 1) by the least mean-square regression method using the Solver utility tool in Excel for Windows, and the parameters K and k_2 were determined (Scandola et al. 1998):

$$V_o = k_2[S]_0 \frac{K[E]_0}{K + [E]_0} \quad (1)$$

Results

Homology modelling

The homology model has only two regions of insertion neither of which are very close to the active enzyme or H172. Furthermore, there are also large regions of conservation between the two sequences (Fig. 1). Hence, we have strong confidence in the developed TtC model. Based on sequence and structural alignment, the TtC catalytic triad consists of S136, D197 and H204, while S58 and Q137 form the oxyanion hole. Like AoC, TtC has an extended groove near the active site constituted by T139, A143, Q147, K154, D155, I157, Y165, T166, Q167, P176 and N177 (Fig. 2). Amongst other important structural features, TtC has two disulfide bonds at C47–C125 and C187–C194, which are conserved amongst most cutinases (e.g. FsC, AoC and AbC). Also a third disulfide bond is predicted by the model between 54 and 69, replacing AoC's third disulfide bond (aligned to positions 73 and 86 in TtC). The two putative glycosylation sites predicted from sequence analysis are located at N127 (NAS) and N195 (NGT). As expected the glycosylation sites are present at the surface, and N195 is in close proximity to the catalytical triad 11.75 A).

Heterologous expression of TtC

TtC was successfully expressed in *K. pastoris* and the bulk production at 4-L scale yielded 200–300 mg/L TtC. However, the expression in yeast leads to glycosylation since TtC has two putative N-linked glycosylation sites. The presence of glycosylation was confirmed by glycopeptide staining of the protein ran on SDS PAGE gel. O-linked glycosylation is very rare in *Pichia pastoris* (Bretthauer and Castellino 1999). Furthermore, the exclusive N-linked glycosylation of TtC was confirmed by deglycosylation using PNGase F which completely deglycosylated TtC. PNGase F is a N-linked glycan-specific deglycosylase (Fig. S1). TtC-NG was successfully produced by expression in *E. coli* Dh5α cells in yields of 20–30 mg/L.

Secondary and tertiary structure analysis

CD wavelength scans in the far UV region (190–240 nm) were recorded to provide information on the secondary structure for both TtC-G and TtC-NG. No significant differences in the CD spectra of TtC-G and TtC-NG were observed. Hence, the presence or absence of the glycans has no apparent effect on the protein conformation. To determine if pH affects the secondary structure of TtC-G and TtC-NG, CD wavelength scans were performed at pH values from 3 to 9 (Fig. 3a, b). The comparison of these CD spectra shows that pH variation did not significantly alter their secondary structure. TtC has two buried tryptophans (W85 and W220). To study the effect of pH on the tertiary structure, an intrinsic tryptophan fluorescence analysis was performed. The maximum fluorescence emission wavelength (λ_{max}) is a function of tryptophan's surrounding environment. The recorded TtC fluorescence spectra for TtC-G and TtC-NG (Fig. 3c, d) showed that the excitation maximum at 340 nm did not significantly vary over the observed pH range. Also, no significant change was observed in the fluorescence intensity. This indicates that the tryptophans remain buried over the pH range from 3 to 9. Similar to CD analysis, the fluorescence analysis results were similar for TtC-G and TtC-NG.

Thermostability analysis

The thermostability of AoC and TtC at varying pH was analyzed by CD temperature scans where the protein melting temperature (T_m) was taken as a measure of the stability. For TtC-G and NG, the pH of optimum thermostability is a narrow region from 4.5 to 5.5 where T_m is 67 and 64 °C for the glycosylated and nonglycosylated forms. In contrast, the optimum pH for AoC thermostability occurs over a broad pH region (5 to 8) where T_m is 61 °C (Fig. 4).

Activity analysis

The activity measurements for TtC-G, TtC-NG and AoC were performed using the polymeric substrates PCL and CA as well as PNPB, a low molar mass model substrate. Cutinases hydrolyze PCL ester groups that link ε-hydroxyhexanoic acid units along the chain and acetate side chains of CA. PCL and CA differ in surface hydrophobicity, where PCL is hydrophobic and CA has a more hydrophilic character due to free hydroxyl and short ester groups. The comparative activity analysis of AoC and TtC on these substrates determined at the optimum pH based on thermal stability analysis (Fig. 4) revealed relatively higher activity of AoC on PCL and TtC for CA (Fig. 5).

Since the optimum pH for thermal stability may not coincide with the optimal pH for activity, the pH-activity profiles at 40 °C for AoC, TtC-G and TtC-NG were determined using PNPB, PCL and CA as substrates. The AoC pH-activity profiles of PNPB and CA as well as a pH optimum at 8.0 are consistent with a previous report on AoC activity for PCL hydrolysis (Baker et al. 2012). In contrast, the pH-activity profiles for TtC were profoundly dependent on the substrate as well as the presence or absence of glycosylation. For PNPB hydrolysis, TtC-G showed a broad pH optimum from pH 5 to pH 8 which is consistent with the observations by Yang et al. (2013). In contrast, TtC-NG showed a small but significant activity loss as the pH decreased from 8 to 5 (Fig. 6a). The pH-activity analysis towards PCL hydrolysis revealed an apparent pH optimum at pH 5 for TtC-G, whereas TtC-NG has a broad pH optimum plateau from pH 5 to pH 8 (Fig. 6b). For CA deacetylation, both TtC-G and TtC-NG show regular increases in their activities at pH values from 5 to 9.0 (Fig. 6c). With the exception of PCL, the activity of glycosylated TtC was lower than the protein in its nonglycosylated form (Table S1).

Polymer hydrolysis kinetics

Enzyme kinetics analyses were performed to understand the significance of substrate binding on enzyme activity for polymeric substrates. The analysis was performed at pH 5 and pH 8 for TtC-G and TtC-NG. However, for AoC, the analysis was performed only at pH 8 as AoC loses its structure and activity at pH 5. All kinetics analyses were performed at 40 °C. The results of PCL hydrolysis and CA deacetylation kinetics analysis are listed in Table 1. AoC showed better adsorption on PCL than TtC, except for TtC at pH 5. However, TtC showed much higher binding than AoC on CA. The binding of TtC-NG on PCL was not affected by pH, while the binding of TtC-G is approximately ten times higher at pH 5 than at pH 8. In contrast, for CA deacetylation, binding for both TtC-G and TtC-NG is not affected by pH but TtC-G binds 1.5 times better than TtC-NG.

Discussion

Structural analysis

The TtC homology model exhibits good similarity as other close homologues for locations of the catalytic triad, oxyanion hole and disulfide bonds. One short insertion is present relative to the AoC template but this is not near the active site. Both AoC and TtC have three disulfides, but the location of one is shifted from 63 to 76 in AoC to 64 to 69 in TtC. This shift may account for the higher stability of TtC relative to AoC. Amongst other features, the specificity of TtC for longer (C4–C5) substrates observed by Yang et al. is consistent with an extended catalytic groove observed near the active site. The presence and significance of a similar extended catalytic groove in AoC are explained elsewhere (Liu et al. 2009).

CD and fluorescence analyses provide information on protein secondary and tertiary structures, respectively. Consequently, they are useful methods for detecting changes in the same due to shifts in medium pH and temperature (Stryer 1968; Kelly et al. 2005). We previously reported that AoC loses its secondary structure under acidic conditions as observed from the CD wavelength scan analysis at lower pHs. This loss of structure leads to the lower enzyme activity of AoC at these pHs (Baker et al. 2012). Similarly, TtC's retention

of activity in acidic pH is consistent with its retention of secondary and the tertiary structure based on CD and fluorescence analyses. Explanation for other trends in the pH-activity profile for TtC-G and TtC-NG are discussed below by considering the protonation state of residues involved in catalysis and substrate binding.

Thermostability

Analysis of the surface charge–charge interaction energies as a function of pH for AoC and TtC was performed using the Tanford–Kirkwood model corrected for solvent accessibility (TKSA) as described previously (Strickler et al. 2006). To account for the relative flexibility of side chains on the surface, an ensemble of 11 structures for each sequence was generated using Modeller, and calculations were performed on each structure individually. The contribution of charge–charge interactions to the Gibbs free energy of unfolding (Gqq) is determined from changes in pKa values of the protein relative to model compounds and assuming that there are no residual charge–charge interactions in the unfolded state. The following values of pKa based on model compounds were used: Asp–4.0; Glu–4.5; Lys–10.6; Arg–12.0; His–6.3; N-term–3.6; C-term–7.7. The averaged Gqq values for AoC and TtC as a function of pH are shown in Fig. 7. The predicted and experimental results (Fig. 4) are in good qualitative agreement which support that electrostatic interactions play an important role in stabilization under acidic conditions. These results suggest that special attention should be paid to surface charge as a means by which the pH-stability profile of AoC and TtC can be 'tuned'.

Previous literature studies show that glycosylation can significantly improve protein stability (Wang et al. 1996; Guo et al. 2008; Zhu et al. 2014). However, the effect of glycosylation is highly dependant on the protein sequence and the location of the glycosylation site (Skropeta 2009). Glycosylation of TtC contributed to small but significant improvement in the T_m. Furthermore, based on the similarity of pH vs stability profiles for TtC-G and TtC-NG, glycosylation did not alter electrostatic interactions (Fig. 4). This work demonstrates that glycosylation site engineering for TtC could be employed to further improve protein stability without altering the pH-activity profile of this enzyme.

Catalytic activity: significance of the substrate binding

Substrate binding is a critically important step in enzyme catalysis at polymeric surfaces. The binding for heterogeneous systems is often expressed as surface adsorption (Hlady and Buijs 1996; Hiraishi et al. 2010b; Khan et al. 2013). Generally, enzyme adsorption onto heterogeneous polymeric substrates is the fast step and the corresponding enzyme-catalyzed reaction is rate limiting (Fox et al. 2012). However, lower binding or the lack of binding has been shown to result in low or no enzyme activity (Hiraishi et al. 2010b). In nature, enzymes that act on heterogeneous substrates are equipped with a binding domain to facilitate substrate binding. Examples include cellulases (Bommarius et al. 2014), poly(3-hydroxybutyrate) depolymerases (Hiraishi et al. 2010a) and xylanases (Khan et al. 2013). Also, engineering the binding domain to improve substrate binding has proved to be an effective tool in enhancing enzyme activity. For example, Hiraishi et al. discovered that small modifications in the binding domain of poly(3-hydroxybutyrate) depolymerases markedly affect its activity based on altered binding (Hiraishi et al. 2010a).

Cutinases are single-domain enzymes, for which the binding should be facilitated by surface residues neighboring the catalytic domain. Substrate binding results in enzyme activity only when the binding is such that the enzyme is properly oriented to facilitate interactions between the enzyme active site and the substrate (Gao et al. 2013). When this latter criteria is fulfilled, then binding is said to be 'productive'. Recently, Acero et al. identified several residues near the active site of *Thermobifida cellulosilytica* which were found to play an important role for PET substrate binding via hydrophobic interactions (Herrero Acero et al. 2013). However, Acero et al. did not perform a quantitative determination of substrate binding to support their hypothesis. Surface plasma resonance (SPR) (Hiraishi et al. 2010a) and quartz crystal microbalance (QCMB) (Kikkawa et al. 2005) are commonly used methods to quantify enzyme surface adsorption. However, these analyses cannot differentiate productive and nonproductive binding.

Since enzyme reaction kinetics is known to provide valuable information on productive binding events (Scandola et al. 1998), polymer hydrolysis kinetic studies were performed herein to explain substrate specificity and TtC's substrate-dependent pH-activity profiles. Indeed, the higher adsorption constants for AoC with PCL, and both glycosylated and nonglycosylated TtC with CA, explain the comparatively higher reactivity for the respective reactions (Fig. 5). The examination of the active site region of both AoC and TtC reveals the presence of surface residues that are consistent with experimentally determined activity data. AoC displays hydrophobic residues near the active site [51–56 PGLLGI] that facilitates enhanced binding on PCL which has a hydrophobic surface (Fig. 8a). In contrast, TtC has hydrophilic surface residues near the active site [61–66 ETGNLGS] (Fig. 8b) consistent with TtC's preference for hydrophilic CA (Fig. 5). Furthermore, the pH-activity profile of TtC on hydrophobic PCL is also explained by the substrate binding. A large difference in the binding constant for TtC-G under alkaline and acidic conditions (Table 1) contributes to its distinct pH-activity profile that decreases sharply with increased pH (Fig. 6b). The pH-dependent hydrophobic interactions where TtC-G's affinity to hydrophobic polyester substrates is enhanced at lower pH values were similarly observed for other hydrophobic polyesters such as polybutylene succinate adipate (data not shown). However, nonglycosylated TtC's binding and k_{cat} values for PCL hydrolysis show little change as the pH varies from 5 to 8. Based on the CD and fluorescence analysis, both TtC-G and TtC-NG have similar structure. Hence, the difference in the pH-binding profiles should be explained based on the involvement in binding of the glycans.

Glycans have been reported to affect substrate binding owing to their hydrophilicity (Hiraishi et al. 2010b). Furthermore, the location of a glycosylation site with respect to the residues involved in substrate binding and glycan size are also important parameters (Chen et al. 2014). TtC is glycosylated at N195 that is in close proximity (12.96 Å) to the active site serine (S-136). Also, characteristic of expression using *Pichia* (Bretthauer and Castellino 1999), TtC is heavily glycosylated with long-chain, mannose-rich glycans. TtC glycosylation was confirmed by SDS PAGE analysis using TtC-G and TtC-G deglycosylated by PNGase F. Comparison of SDS PAGE gel bands with glycopeptide and Coomassie blue staining for the glycosylated and deglycosylated proteins shows that glycosylated TtC appears at relatively higher molecular weights and has multiple bands consistent with heterogeneous glycosylation (Fig. S1). Previous work with cellulases showed that the

presence of long-chain glycans negatively affected enzyme activity (Chen et al. 2014). In the case of TtC, the glycosylated form is less active than its nonglycosylated counterpart for PNPB hydrolysis (Table S1), which indicates that the steric hinderance of the glycan interferes with its activity for PNPB hydrolysis. In the case of insoluble polymeric substrates, the steric effect of a glycan can also interfere in substrate binding. The substrate binding of TtC is influenced by protein-substrate interactions which are pH dependent. Thus, the difference between the pH-activity profiles of TtC-G and TtC-NG for PCL hydrolysis is likely due to the changes in glycan orientation or conformation relative to the protein and substrate over the pH 5–8 region. Hence, this logic requires the identification of an amino acid residue whose protonation state is variable over this pH range and is located in close proximity to H195. The study of the enzyme structure reveals that H172 is not part of the catalytic triad (S136, D191, H204) and is 10.2 Å from the glycosylation site. While H172 is located 16.51 Å from the active site serine, it is found along the substrate-binding groove (Fig. 9)]. Also, histidine has a pKa of ~6 so it is charged (protonated) at pH 5 and noncharged at pH 8. Thus, we believe that at as the pH increases to 8, H172 transitions to the noncharged state that changes in glycan orientation or conformation that negatively affects effective protein-substrate interactions that lead to hydrolysis reactions. It follows that the opposite occurs as the pH of the reaction medium decreases from pH 8 to 6. Based on the current homology model of TtC, orientations of H172 and N195 cannot be predicted owing to a poor modelling confidence in this region. Moreover, these residues are present on the unstructured loop region (Fig. 9). To confirm this steric effect imposed by the glycan, the TtC variant N195Q was synthesized that is not glycosylated at N195 (Online resource 1). Indeed, TtC-N195Q displayed a pH-activity profile that closely resembles that of TTC-NG (Fig. 10). However, the specific activity of TtC-N195Q was found to be lower than both TtC-G and TtC-NG. This loss of activity could be attributed to the small yet significant structural changes caused by the N195Q mutation near the active site. Future work will look more closely to define on a molecular level the precise nature of protein-glycan-substrate interactions.

Unlike PCL hydrolysis, CA deacetylation by both TtC-G and TtC-NG showed similar pH-activity profiles. Thus, protonation of H172 does not appear to play an important role for TtC-CA binding. The optimum pH for TtC deacetylation of CA is greater than 8. This is likely due to that substrate binding is not a rate-limiting step for CA deacetylation and the activity is primarily governed by the actual turnovers. The K_{cat} values for both TtC-G and TtC-NG were found to be significantly higher (>2×) at pH 8 than at pH 5, although substrate binding was hardly affected by pH. Glycosylation was expected to improve the binding of TtC to CA due to corresponding hydrophilic interactions between the glycan at N195 and CA. Indeed, binding with CA at both pH 5 and 8 is higher for the glycosylated protein (Table 1). However, the activity of TtC-G is lower than that of TtC-NG. This may be due to the glycan length (discussed above) that sterically constrains access of CA acetate groups to the active site.

The above discussion demonstrates that glycosylated TtC has higher thermal stability but is less active than its nonglycosylated form. This difference in activity as a function of glycosylation is more evident for PCL, the hydrophobic substrate. Nevertheless, natural TtC exists in the glycosylated form and acts on cutin, a hydrophobic substrate cutin. However,

the differences in the glycosylation pattern in *P. pastoris* (long-chain, mannose-rich glycans) vs the native glycans of *T. terrestis* may provide an explanation for this inconsistency. Furthermore, studies were not performed herein on the activity of TtC on cutin. Future work will further explore how glycosylation site engineering can be employed to optimize enzyme activity and stability.

Supplementary Material

Refer to Web version on PubMed Central for supplementary material.

Acknowledgments

References

Badenes SM, Lemos F, Cabral JMS. Transesterification of oil mixtures catalyzed by microencapsulated cutinase in reversed micelles. Biotechnol Lett. 2010; 32:399–403. [PubMed: 19943181]

Baker PJ, Poultney C, Liu Z, Gross R, Montclare JK. Identification and comparison of cutinases for synthetic polyester degradation. Appl Microbiol Biotechnol. 2012; 93:229–240. [PubMed: 21713515]

Banás P, Walter NG, Sponer J, Otyepka M. Protonation states of the key active site residues and structural dynamics of the glmS riboswitch as revealed by molecular dynamics. J Phys Chem B. 2010; 114:8701–8712. [PubMed: 20536206]

Beckham GT, Dai Z, Matthews JF, Momany M, Payne CM, Adney WS, Baker SE, Himmel ME. Harnessing glycosylation to improve cellulase activity. Curr Opin Biotechnol. 2012; 23:338–345. [PubMed: 22186222]

Bhardwaj H, Gupta R, Tiwari A. Communities of microbial enzymes associated with biodegradation of plastics. J Polym Environ. 2012; 21:575–579.

Bommarius AS, Sohn M, Kang Y, Lee JH, Realff MJ. Protein engineering of cellulases. Curr Opin Biotechnol. 2014; 29:139–145. [PubMed: 24794535]

Bretthauer RK, Castellino FJ. Glycosylation of *Pichia pastoris*-derived proteins. Biotechnol Appl Biochem. 1999; 30(Pt 3):193–200. [PubMed: 10574687]

Chan C-H, Wilbanks CC, Makhatadze GI, Wong K-B. Electrostatic contribution of surface charge residues to the stability of a thermophilic protein: benchmarking experimental and predicted pKa values. PLoS One. 2012; 7:e30296. [PubMed: 22279578]

Chen L, Drake MR, Resch MG, Greene ER, Himmel ME, Chaffey PK, Beckham GT, Tan Z. Specificity of O-glycosylation in enhancing the stability and cellulose binding affinity of Family 1 carbohydrate-binding modules. Proc Natl Acad Sci U S A. 2014; 111:7612–7617. [PubMed: 24821760]

Chen S, Su L, Chen J, Wu J. Cutinase: characteristics, preparation, and application. Biotechnol Adv. 2013; 31:1754–1767. [PubMed: 24055682]

De Barros DPC, Azevedo AM, Cabral JMS, Fonseca LP. Optimization of flavor esters synthesis by Fusarium solani pisi cutinase. J Food Biochem. 2012; 36:275–284.

Dutta K, Sen S, Veeranki VD. Production, characterization and applications of microbial cutinases. Process Biochem. 2009; 44:127–134.

Fox JM, Levine SE, Clark DS, Blanch HW. Initial- and processive-cut products reveal cellobiohydrolase rate limitations and the role of companion enzymes. Biochemistry. 2012; 51:442–452. [PubMed: 22103405]

Gao D, Chundawat SPS, Sethi A, Balan V, Gnanakaran S, Dale BE. Increased enzyme binding to substrate is not necessary for more efficient cellulose hydrolysis. Proc Natl Acad Sci U S A. 2013; 110:10922–10927. [PubMed: 23784776]

García-Mayoral MF, del Pozo AM, Campos-Olivas R, Gavilanes JG, Santoro J, Rico M, Laurents DV, Bruix M. pH-Dependent conformational stability of the ribotoxin alpha-sarcin and four active site charge substitution variants. Biochemistry. 2006; 45:13705–13718. [PubMed: 17105190]

Gribenko AV, Patel MM, Liu J, SA MC, Wang C, Makhatadze GI. Rational stabilization of enzymes by computational redesign of surface charge-charge interactions. Proc Natl Acad Sci U S A. 2009; 106:2601–2606. [PubMed: 19196981]

Guebitz GM, Cavaco-Paulo A. Enzymes go big: surface hydrolysis and functionalization of synthetic polymers. Trends Biotechnol. 2008; 26:32–38. [PubMed: 18037176]

Guo M, Hang H, Zhu T, Zhuang Y, Chu J, Zhang S. Effect of glycosylation on biochemical characterization of recombinant phytase expressed in Pichia pastoris. Enzym Microb Technol. 2008; 42:340–345.

Herrero Acero E, Ribitsch D, Dellacher A, Zitzenbacher S, Marold A, Steinkellner G, Gruber K, Schwab H, Guebitz GM. Surface engineering of a cutinase from *Thermobifida cellulosilytica* for improved polyester hydrolysis. Biotechnol Bioeng. 2013; 110:2581–2590. [PubMed: 23592055]

Hiraishi T, Komiya N, Maeda M. Y443F mutation in the substrate-binding domain of extracellular PHB depolymerase enhances its PHB adsorption and disruption abilities. Polym Degrad Stab. 2010a; 95:1370–1374.

Hiraishi T, Komiya N, Matsumoto N, Abe H, Fujita M, Maeda M. Degradation and adsorption characteristics of PHB depolymerase as revealed by kinetics of mutant enzymes with amino acid substitution in substrate-binding domain. Biomacromolecules. 2010b; 11:113–119. [PubMed: 20058938]

Hlady V, Buijs J. Protein adsorption on solid surfaces. Curr Opin Biotechnol. 1996; 7:72–77. [PubMed: 8791316]

Horng J-C, Cho J-H, Raleigh DP. Analysis of the pH-dependent folding and stability of histidine point mutants allows characterization of the denatured state and transition state for protein folding. J Mol Biol. 2005; 345:163–173. [PubMed: 15567419]

Hu X, Thumarat U, Zhang X, Tang M, Kawai F. Diversity of polyester-degrading bacteria in compost and molecular analysis of a thermoactive esterase from Thermobifida alba AHK119. Appl Microbiol Biotechnol. 2010; 87:771–779. [PubMed: 20393707]

Hunsen M, Azim A, Mang H, Wallner SR, Ronkvist A, Xie W, Gross RA. A cutinase with polyester synthesis activity. Macromolecules. 2007; 40:148–150.

Jehle S, Rajagopal P, Bardiaux B, Markovic S, Kühne R, Stout JR, Higman VA, Klevit RE, van Rossum B-J, Oschkinat H. Solid-state NMR and SAXS studies provide a structural basis for the activation of alphaB-crystallin oligomers. Nat Struct Mol Biol. 2010; 17:1037–1042. [PubMed: 20802487]

Kawai F, Oda M, Tamashiro T, Waku T, Tanaka N, Yamamoto M, Mizushima H, Miyakawa T, Tanokura M. A novel Ca(2+)-activated, thermostabilized polyesterase capable of hydrolyzing polyethylene terephthalate from *Saccharomonospora viridis* AHK190. Appl Microbiol Biotechnol. 2014; 98:10053–10064. [PubMed: 24929560]

Kelly SM, Jess TJ, Price NC. How to study proteins by circular dichroism. Biochim Biophys Acta. 2005; 1751:119–139. [PubMed: 16027053]

Khan MIM, Sajjad M, Sadaf S, Zafar R, Niazi UHK, Akhtar MW. The nature of the carbohydrate binding module determines the catalytic efficiency of xylanase Z of *Clostridium thermocellum.* J Biotechnol. 2013; 168:403–408. [PubMed: 24095983]

Kikkawa Y, Yamashita K, Hiraishi T, Kanesato M, Doi Y. Dynamic adsoption behavior of poly(3-hydroxybutyrate) depolymerase onto polyester surface investigated by QCM and AFM. Biomacromolecules. 2005; 6:2084–2090. [PubMed: 16004448]

Köller W, Kolattukudy PE. Mechanism of action of cutinase: chemical modification of the catalytic triad characteristic for serine hydrolases. Biochemistry. 1982; 21:3083–3090. [PubMed: 6809046]

Lin-Cereghino J, Wong WW, Xiong S, Giang W, Luong LT, Vu J, Johnson SD, Lin-Cereghino GP. Condensed protocol for competent cell preparation and transformation of the methylotrophic yeast *Pichia pastoris*. Biotechniques. 2005; 38:44, 46, 48. [PubMed: 15679083]

Liu Z, Gosser Y, Baker PJ, Ravee Y, Lu Z, Alemu G, Li H, Butterfoss GL, Kong X-P, Gross R, Montclare JK. Structural and functional studies of *Aspergillus oryzae* cutinase: enhanced thermostability and hydrolytic activity of synthetic ester and polyester degradation. J Am Chem Soc. 2009; 131:15711–15716. [PubMed: 19810726]

Martinez C, De Geus P, Lauwereys M, Matthyssens G, Cambillau C. *Fusarium solani* cutinase is a lipolytic enzyme with a catalytic serine accessible to solvent. Nature. 1992; 356:615–618. [PubMed: 1560844]

Martinez C, Nicolas A, van Tilbeurgh H, Egloff MP, Cudrey C, Verger R, Cambillau C. Cutinase, a lipolytic enzyme with a preformed oxyanion hole. Biochemistry. 1994; 33:83–89. [PubMed: 8286366]

Matamá T, Araújo R, Gübitz GM, Casal M, Cavaco-Paulo A. Functionalization of cellulose acetate fibers with engineered cutinases. Biotechnol Prog. 2009; 26:636–643. [PubMed: 20014432]

Mazzini A, Polverini E, Parisi M, Sorbi RT, Favilla R. Dissociation and unfolding of bovine odorant binding protein at acidic pH. J Struct Biol. 2007; 159:82–91. DOI: 10.1016/j.jsb.2007.02.007 [PubMed: 17428681]

Mueller R-J. Biological degradation of synthetic polyesters—enzymes as potential catalysts for polyester recycling. Process Biochem. 2006; 41:2124–2128.

Neves-Petersen MT, Petersen EI, Fojan P, Noronha M, Madsen RG, Petersen SB. Engineering the pH-optimum of a triglyceride lipase: from predictions based on electrostatic computations to experimental results. J Biotechnol. 2001; 87:225–254. [PubMed: 11334666]

Nyyssölä A, Pihlajaniemi V, Häkkinen M, Kontkanen H, Saloheimo M, Nakari-Setälä T. Cloning and characterization of a novel acidic cutinase from *Sirococcus conigenus*. Appl Microbiol Biotechnol. 2014; 98:3639–3650. [PubMed: 24121867]

Nyyssölä A, Pihlajaniemi V, Järvinen R, Mikander S, Kontkanen H, Kruus K, Kallio H, Buchert J. Screening of microbes for novel acidic cutinases and cloning and expression of an acidic cutinase from *Aspergillus niger* CBS 513.88. Enzyme and Microbial Technology. 2013; 52:272–278. [PubMed: 23540930]

Payne CM, Resch MG, Chen L, Crowley MF, Himmel ME, Taylor LE, Sandgren M, Ståhlberg J, Stals I, Tan Z, Beckham GT. Glycosylated linkers in multimodular lignocellulose-degrading enzymes dynamically bind to cellulose. Proc Natl Acad Sci U S A. 2013; 110:14646–14651. [PubMed: 23959893]

Purdy RE, Kolattukudy PE. Hydrolysis of plant cuticle by plant pathogens. Properties of cutinase I, cutinase II, and a nonspecific esterase isolated from *Fusarium solani* pisi. Biochemistry. 1975; 14:2832–2840. [PubMed: 239740]

Rhee JK, Ahn DG, Kim YG, Oh JW. New thermophilic and thermostable esterase with sequence similarity to the hormone-sensitive lipase family, cloned from a metagenomic library. Appl Environ Microbiol. 2005; 71:817–825. [PubMed: 15691936]

Ronkvist ÅM, Lu W, Feder D, Gross RA. Cutinase-catalyzed deacetylation of poly(vinyl acetate). Macromolecules. 2009a; 42:6086–6097.

Ronkvist ÅM, Xie W, Lu W, Gross RA. Cutinase-catalyzed hydrolysis of poly(ethylene terephthalate). Macromolecules. 2009b; 42:5128–5138.

Roth C, Wei R, Oeser T, Then J, Föllner C, Zimmermann W, Sträter N. Structural and functional studies on a thermostable polyethylene terephthalate degrading hydrolase from *Thermobifida fusca*. Appl Microbiol Biotechnol. 2014; 98:7815–7823. [PubMed: 24728714]

Sampogna RV, Honig B. Environmental effects on the protonation states of active site residues in bacteriorhodopsin. Biophys J. 1994; 66:1341–1352. [PubMed: 8061190]

Scandola M, Focarete ML, Frisoni G. Simple kinetic model for the heterogeneous enzymatic hydrolysis of natural poly (3-hydroxybutyrate). Macromolecules. 1998; 31:3846–3851.

Skropeta D. The effect of individual N-glycans on enzyme activity. Bioorganic Med Chem. 2009; 17:2645–2653.

Strickler SS, Gribenko AV, Gribenko AV, Keiffer TR, Tomlinson J, Reihle T, Loladze VV, Makhatadze GI, Pennsyl V. Accelerated publications protein stability and surface electrostatics: a charged relationship. Biochemistry. 2006; 45(9):2761–1766. [PubMed: 16503630]

Stryer L. Fluorescence spectroscopy of proteins. Science. 1968; 162:526–533. [PubMed: 5706935]

Sulaiman S, Yamato S, Kanaya E, Kim J-J, Koga Y, Takano K, Kanaya S. Isolation of a novel cutinase homolog with polyethylene terephthalate-degrading activity from leaf-branch compost by using a metagenomic approach. Appl Environ Microbiol. 2012; 78:1556–1562. [PubMed: 22194294]

Sulaiman S, You D-J, Kanaya E, Koga Y, Kanaya S. Crystal structure and thermodynamic and kinetic stability of metagenome-derived LC-cutinase. Biochemistry. 2014; 53:1858–1869. [PubMed: 24593046]

Sussman F, Villaverde CM, Dominguez JL, Danielson UH. On the active site protonation state in aspartic proteases: implications for drug design. Curr Pharm Des. 2013; 19(23):4257–4275. [PubMed: 23170891]

Talley K, Alexov E. On the pH-optimum of activity and stability of proteins. Proteins. 2010; 78:2699–2706. [PubMed: 20589630]

Wang C, Eufemi M, Turano C, Giartosio A. Influence of the carbohydrate moiety on the stability of glycoproteins. Biochemistry. 1996; 35:7299–7307. [PubMed: 8652506]

Yamato I, Rosenbusch JP. Dependence on pH of substrate binding to lactose carrier in *Escherichia coli* cytooplasmic membranes. FEBS Lett. 1983; 151:102–104. [PubMed: 6297984]

Yang S, Xu H, Yan Q, Liu Y, Zhou P, Jiang Z. A low molecular mass cutinase of *Thielavia terrestris* efficiently hydrolyzes poly(esters). J Ind Microbiol Biotechnol. 2013; 40:217–226. [PubMed: 23271406]

Zacharius RM, Zell TE, Morrison JH, Woodlock JJ. Glycoprotein staining following electrophoresis on acrylamide gels. Anal Biochem. 1969; 30:148–152. [PubMed: 4183001]

Zhu J, Liu H, Zhang J, Wang P, Liu S, Liu G, Wu L. Effects of Asn-33 glycosylation on the thermostability of Thermomyces lanuginosus lipase. J Appl Microbiol. 2014; 117:151–159. [PubMed: 24724829]
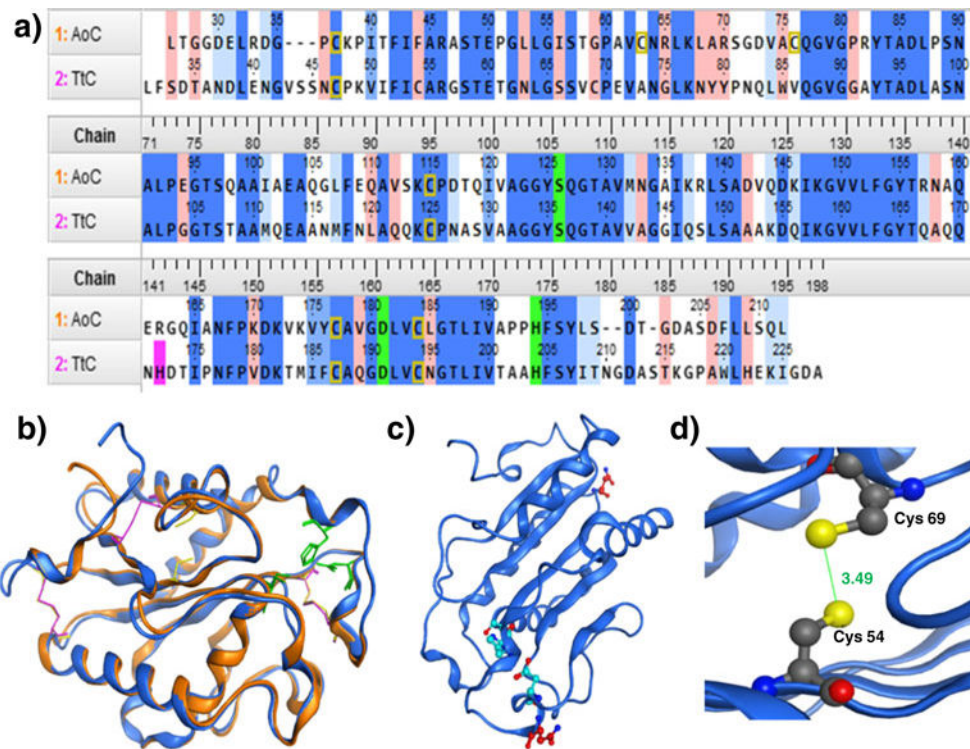
Fig. 1.

a Sequence alignment of AoC and TtC. *Blue* indicates conserved residues, *light blue* is similar, and *pink* is dissimilar. Active site residues are colored *green*, and H172 is shown in *purple*. Cysteines are boxed in *yellow*. **b** Structure overlay of TtC and AoC generated from the homology model and crystal structure 3GBS, respectively. *Blue ribbon* TtC, *yellow* disulfides, *orange ribbon* AoC, *purple* disulfides. **c** Location of glycosylation sites in TtC (*red*) relative to active site (*cyan*). **d** Third putative disulfide bond in TtC
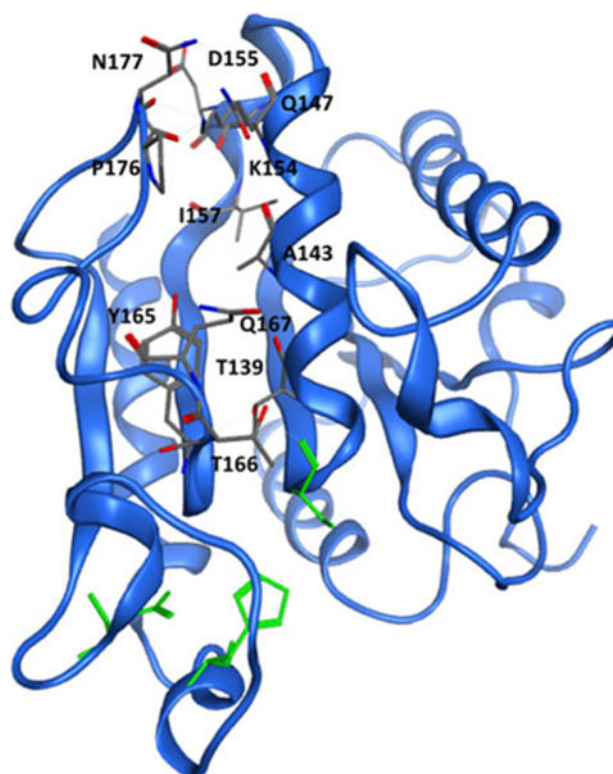
Fig. 2.
Extended catalytic groove near the active site (*green*) of TtC
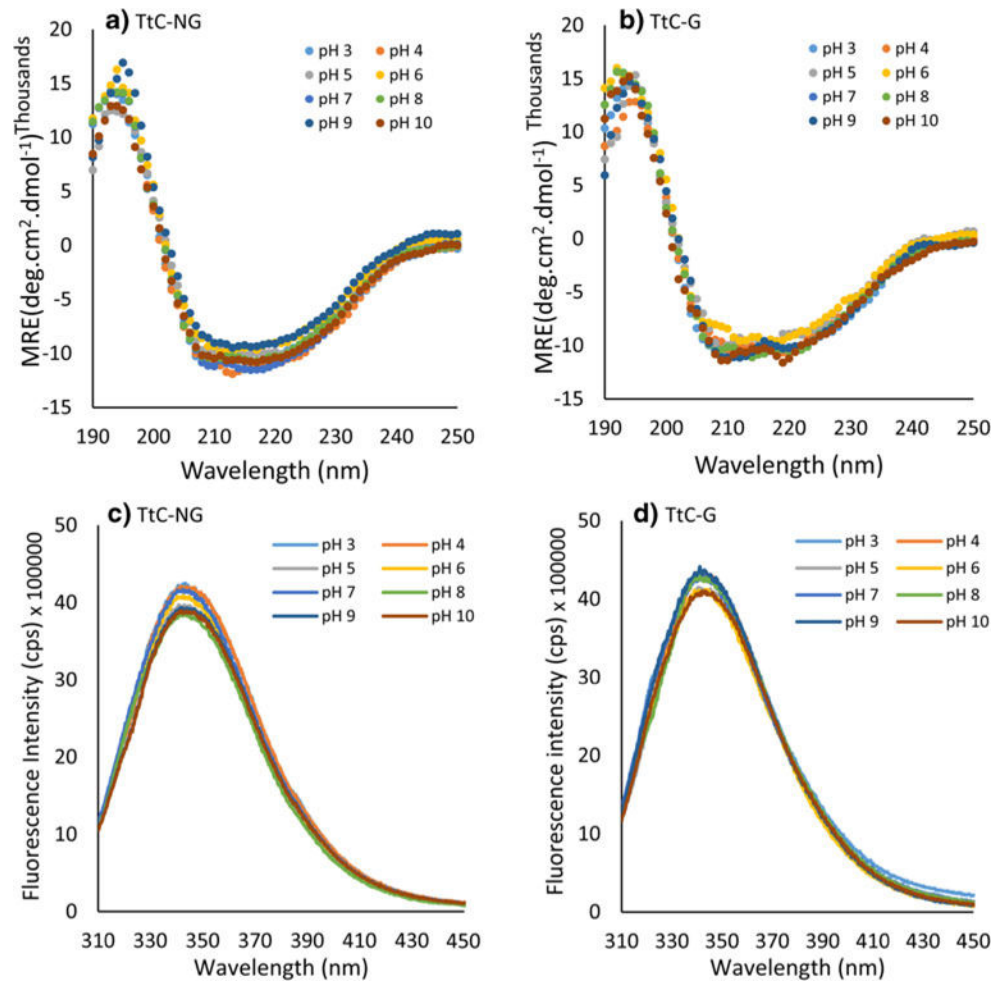
Fig. 3.
Secondary structure analysis by CD wavelength scans (**a** and **b**) and intrinsic tryptophan fluorescence analysis (**c** and **d**) of TtC-G and TtC-NG as a function of pH
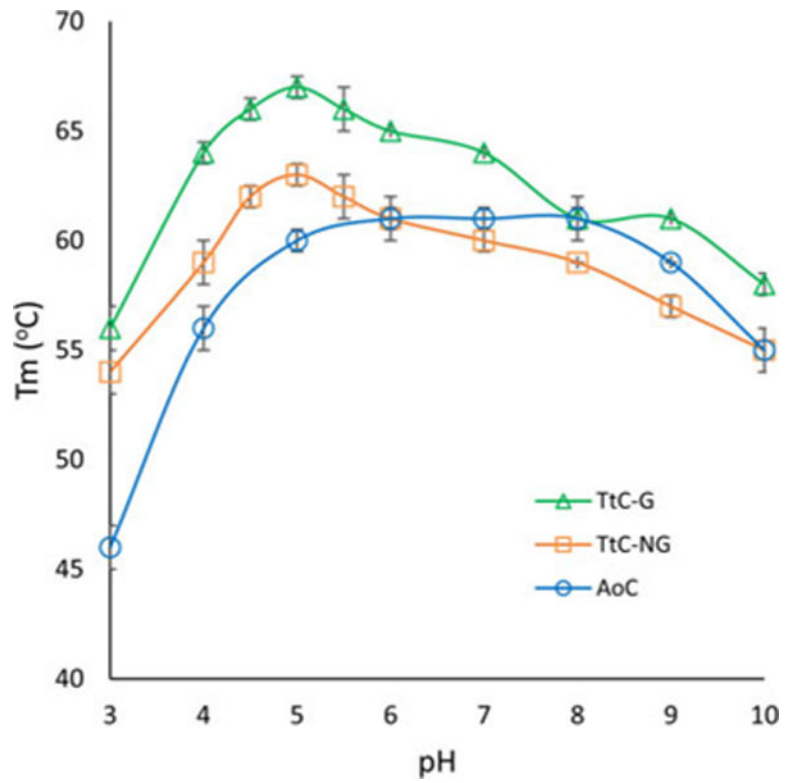
Fig. 4.
Thermostability of AoC, TtC-G and TtC-NG as a function of pH determined by CD temperature scans. *Continuous lines* are used to guide the eyes
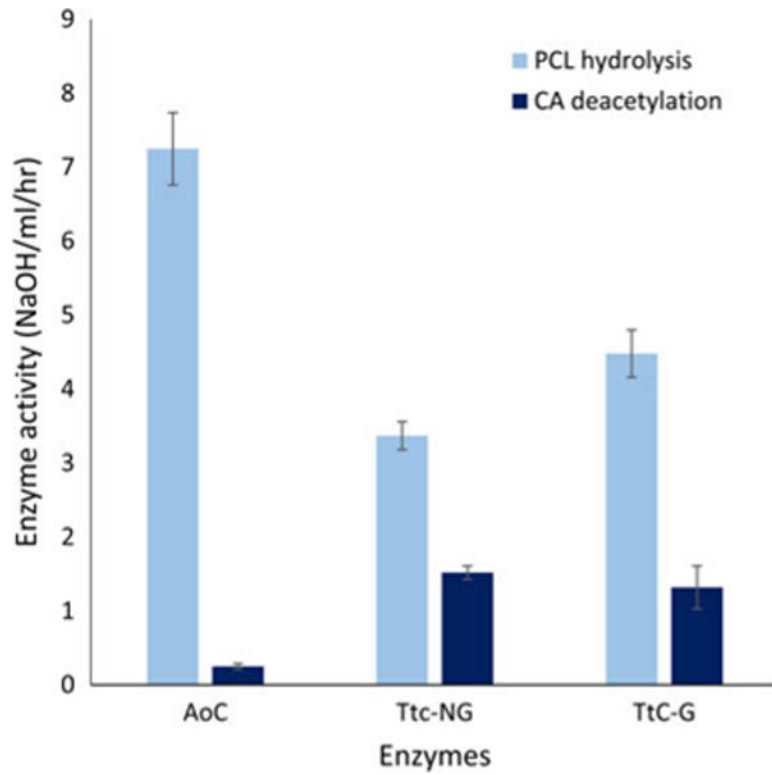
Fig. 5.
Activity analysis of AoC, TtC-G and TtC-NG on cellulose acetate (CA) and polycaprolactone (PCL). Measurements were performed using 2 cm^2/mL of the polymeric substrates and 100 nM of the enzymes at 40 °C and pH 8 for AoC and pH 5 for TtC)
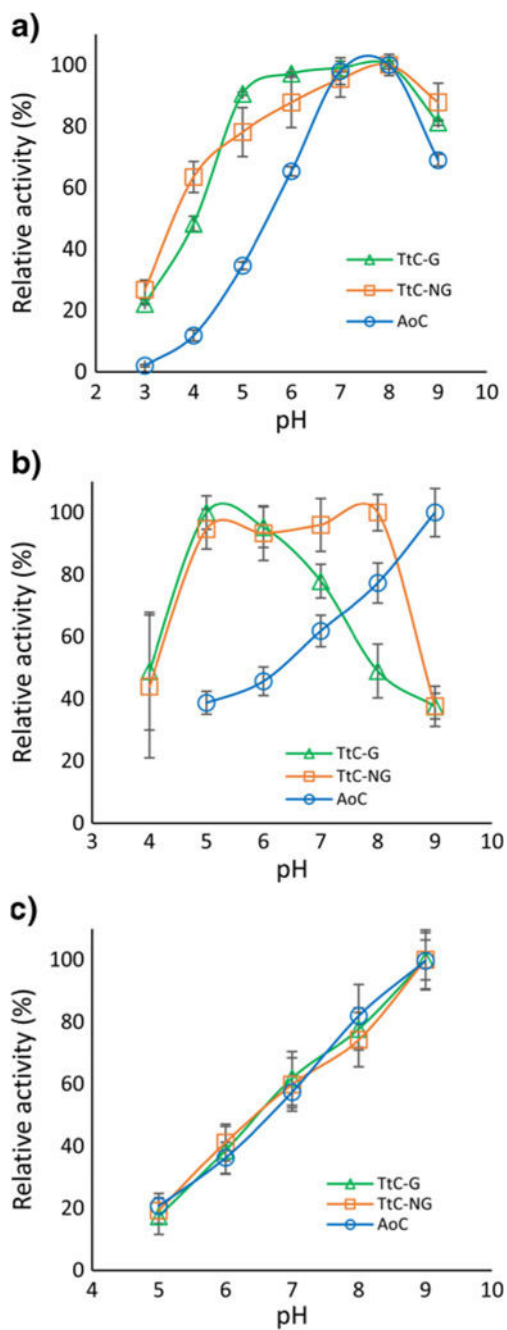
Fig. 6.
Relationships of pH activity for AoC, TtC-G and TtC-NG on **a** PNPB, **b** PCL and **c** CA. The analyses were performed at 40 °C for PCL hydrolysis and CA deacetylation whereas PNPB hydrolysis was performed at 25 °C. *Continuous lines* are used to guide the eyes For clarity, relative activity values are given here instead of absolute activities. Values of absolute activity are listed in the Table S1
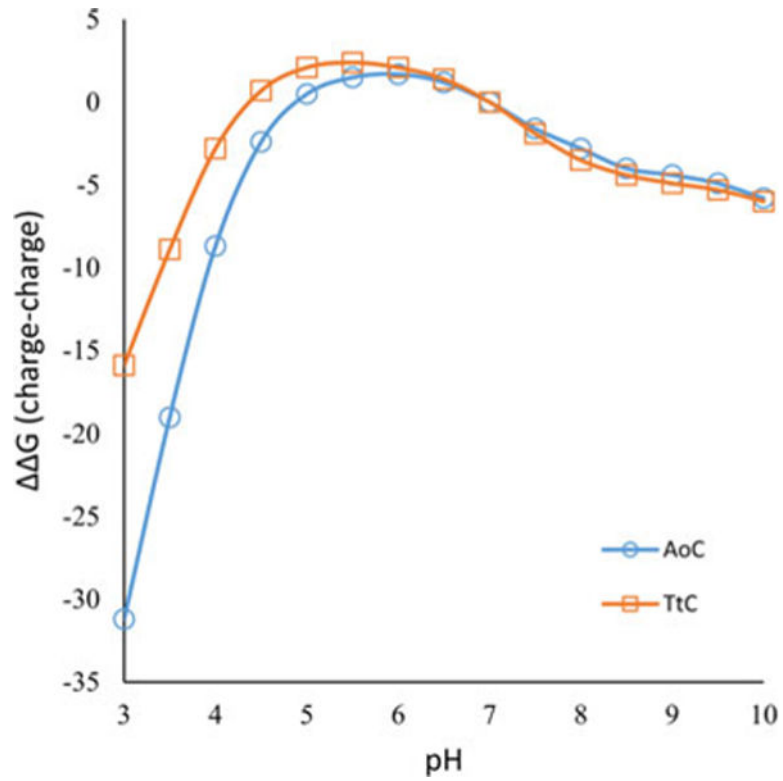
Fig. 7.
Surface charge calculation (contribution of the charge interaction to the Gibbs free energy of unfolding) for AOC and TtC
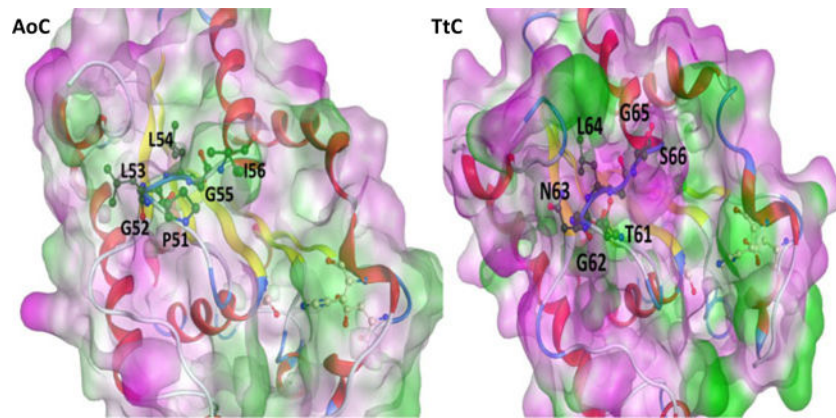
Fig. 8.
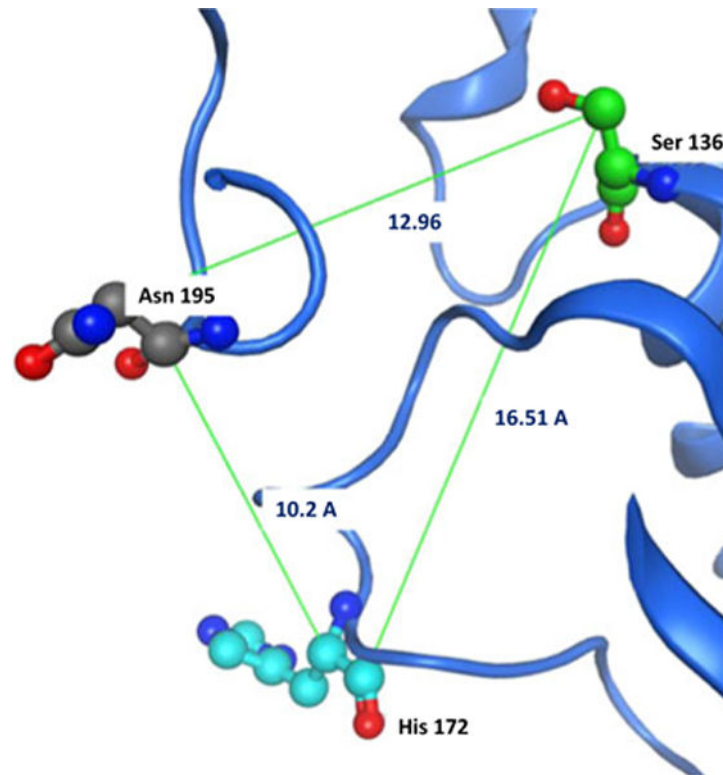Surface analysis of AoC(L) and TtC (R). *Green* hydrophobic, *purple* hydrophilic

Fig. 9.
Histidine-glycan hypothesis: orientation and the distance of H172 and N195 form the catalytic serine S136
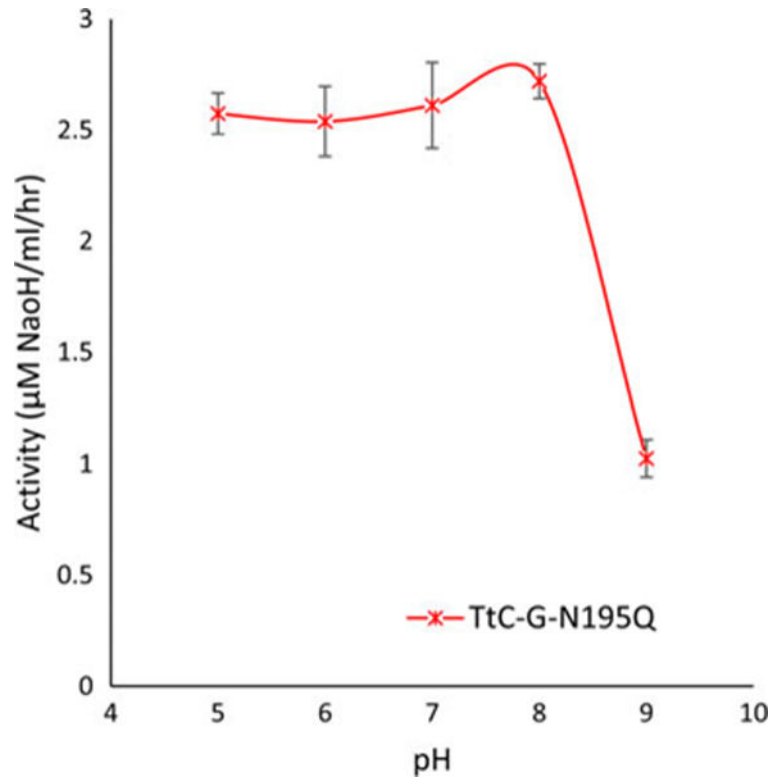
Fig. 10.
pH-activity analysis of TtC-G-N195Q. *Continuous lines* are used to guide the eyes

Table 1

Enzyme kinetic analysis at 40 °C of AoC, TtC-G and TtC-NG for PCL hydrolysis and CA deacetylation

Enzyme	Substrate	PCL		CA	
	pH	K (μM)	k_{cat} (μmol/cm²/h)	K (μM⁻¹)	k_{cat} (μmol/cm²/h)
TtC-G	5	17.07	5.6	3.8	1.3
	8	1.6	6.7	4.2	2.66
TtC-NG	5	3.7	6.4	2.75	1.78
	8	3.3	7.7	2.42	3.64
AoC	8	7.13	29.4	0.19	4.86